Wave Digital Filter Adaptors for Arbitrary Topologies and Multiport Linear Elements

WAVE DIGITAL FILTER ADAPTORS FOR ARBITRARY TOPOLOGIES AND MULTIPORT LINEAR ELEMENTS

Kurt James Werner, Julius O. Smith III, Jonathan S. Abel

Center for Computer Research in Music and Acoustics (CCRMA), Stanford University
660 Lomita Drive, Stanford, CA 94305, USA
[kwerner|jos|abel]@ccrma.stanford.edu

ABSTRACT

We present a Modified-Nodal-Analysis-derived method for developing Wave Digital Filter (WDF) adaptors corresponding to complicated (non-series/parallel) topologies that may include multiport linear elements (e.g. controlled sources and transformers). A second method resolves noncomputable (non-tree-like) arrangements of series/parallel adaptors. As with the familiar 3-port series and parallel adaptors, one port of each derived adaptor may be rendered reflection-free, making it acceptable for inclusion in a standard WDF tree. With these techniques, the class of acceptable reference circuits for WDF modeling is greatly expanded. This is demonstrated by case studies on circuits which were previously intractable with WDF methods: the Bassman tone stack and Tube Screamer tone/volume stage.

1. INTRODUCTION

The Wave Digital Filter (WDF) concept [1] provides an elegant framework for creating digital models of analog reference circuits (or any lumped reference system). However, the class of reference circuits which are tractable with WDF techniques is very small. Specifically, reference circuits with complicated topologies (those that can't be decomposed entirely into series and parallel connections) and/or multiport linear elements (transformers, controlled sources, operational amplifiers, etc.) are *not* accommodated *in general* by known techniques.

In this work, we focus on expanding the class of tractable *linear* reference circuits to include these problematic cases. Although these elements may be accomodated by known techniques in specific configurations, the situations where they are problematic are *not* rare edge cases. For instance, bridged-T networks [2] are commonly present in guitar tone stack circuits [3, 4] and analog drum machine circuits [5–7]. Operational amplifiers are often used in complicated feedback arrangements which thwart WDF modeling except under specific circumstances [8]. This work addresses a need for simple adaptor derivation procedures suitable for *any* topology which may arise in a reference circuit. To that end, we'll emphasize methodical and even automatable "stamp" techniques, well-known in Modified Nodal Analysis (MNA) [9–12].

Researchers have primarily targeted the well-known restriction of WDFs to reference circuits with a single nonlinearity [13]. Since musical circuits in general may contain *many* nonlinearities, physical modeling / virtual analog researchers have focused on trying to extend this result to the case of multiple and multiport nonlinearities. However, we argue that limitations on WDF reference circuit topologies are just as problematic. In a companion paper [14], we'll review treatments of nonlinearities in WDFs and show how the resolution of topological issues presented in this paper enable novel treatments of reference circuits with multiple/multiport nonlinear elements.

In §2, we review relevant previous work. Two novel methods for deriving adaptor structures are given in §§3–4. Case studies on the Fender Bassman tone stack and Tube Screamer tone/volume stage are given in §5. Both circuits have problematic topologies which render them intractable with classical WDF techniques—their simulation demonstrates the success of our methods.

2. PREVIOUS WORK

In the early 1970s, Alfred Fettweis formulated the WDF framework as a technique for designing digital filter structures that mimic the properties of analog reference circuits, which had well-studied behavior and well-established design principles [15, 16]. The analog reference circuits of interest commonly had ladder [17] or lattice [18] structure. Hence, it is not surprising that when Fettweis and Meerkötter formalized the concept of a WDF adaptor, they focused on series and parallel connections [19].

When Fettweis published his omnibus 1986 article "Wave Digital Filters: Theory and Practice" [1], the WDF formalism had reached a high level of maturity. This included extensions to the multidimensional case which led to uses of WDFs as solvers of partial differential equations [20]. Today, in physical modeling [21] and virtual analog, WDFs are an active research area. Researchers in these fields aim to mimic the behavior of musical circuitry, such as guitar amplifiers and effect pedals. WDFs are attractive for this application, but the range of reference circuits that the framework can be applied to is significantly restricted.

Classical WDF methods are applicable *only* to circuits whose topologies can be decomposed into series and parallel connections [19]. Although the significance of this limitation is only rarely acknowledged, it was noted by Martens and Meerkötter as early as 1976 [22]. Fränken *et al.* [23, 24] used formal graph-theoretic methods to generate adaptor structures from circuits with complicated topologies. Their work yields insights about the existence and implications of complicated topologies and ideal transformers [23, 24], though without presenting a method for deriving the actual scattering behavior of the resulting $\mathcal{R}$*-type* adaptors.[1]

Recently, Paiva *et al.* studied operational amplifiers (op-amps) in a WDF context [8], showing how circuits with an op-amp differential amplifier topology can be treated as a feedforward cascade of controlled sources—we can consider this an instance of the "leaf–leaf connection" discussed by De Sanctis and Sarti [26].

[1] Meerkötter and Fränken furthermore propose techniques for factorizing scattering matrices to reduce computational costs [25], but again this cannot be applied in a WDF context without knowledge of the scattering behavior of these adaptors.

Although it is clear that a generalization of their technique would be applicable to some other op-amp topologies, there are cases where the relationships among controlled sources will create inadmissible feedback loops.

Some researchers have shown examples of circuits with complicated topologies which, if we insist on only using classical 3-port series and parallel adaptors, result in non-treelike (and hence noncomputable) *ring structures* [2, 27]. Schwerdtfeger and Kummert studied methods for iteratively resolving such ring structures at runtime, based on contractivity properties of WDF elements [2].

3. METHOD ONE: MNA

Here we present a novel method, based on graph-theoretic views of WDF adaptor structures, for finding the scattering matrix of a WDF adaptor with arbitrary topology that may include absorbed linear multiport elements. A special case without any linear multiport elements was briefly presented in [28]. Although this may seem a violation of the modularity goal of WDFs, absorbing WDF elements into adaptors to ease realizability issues is as old as WDFs themselves—Fettweis' resistive voltage (current) source [16] can be considered merely a voltage (current) source and a resistor absorbed into a 3-port series (parallel) adaptor.

Given a reference circuit, which may contain linear multiport elements and complicated topologies, the first step of our method is to find a suitable WDF adaptor structure. It is possible to accomplish this by inspection, but more convenient to apply the method of Fränken *et al.* [23, 24]. According to this method, a connected graph representing the reference circuit is formed, where graph nodes correspond to circuit nodes and graph edges correspond to ports in the circuits, i.e., these graph edges correspond to bipole circuit elements (resistors, capacitors, inductors, etc.) or ports of a linear multiport element (transformer, controlled source, etc.).

Then, standard graph separation algorithms which find "split components" are used to decompose the connected graph into a tree structure: the *SPQR tree*. For realizability reasons, we must ensure that these graph separation algorithms will not separate edges that correspond to a multiport circuit element. This can be avoided by pre-processing the graph structure with so-called *replacement graphs* before applying a separation algorithm [24].[2] A minimal suitable replacement graph includes the addition of 3 fictitious nodes to each multiport element, and fictitious edges connecting each one of them to every original node in the multiport element; this is sufficient to ensure that graph separation algorithms will not break apart the multiport linear element.

In the SPQR tree, nodes represent topological entities in the graph with detected split components, and edges represent virtual edges in the split components. $\mathcal{S}$, $\mathcal{P}$, and $\mathcal{R}$ nodes correspond directly to familiar **S**eries adaptors, **P**arallel adaptors, and the less well-known family of **R**igid or "strongly connected" adaptors. $\mathcal{Q}$ nodes correspond to single component ports. This process highlights the fact that series and parallel adaptors are *not* sufficient to represent all linear circuit topologies, not even those without multiport elements. A result of using replacement graphs, multiport linear elements will commonly "clump up" inside of $\mathcal{R}$-type nodes. The idea of sources absorbed into adaptors is not necessarily new [26], but generalizing the concept in light of formal graph decomposition methods is crucial to our approach.

[2] An example is given in §5.2.

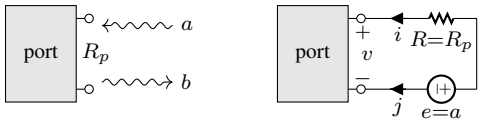

(a) *Wave domain.* (b) *Kirchhoff domain.*

Figure 1: *Instantaneous Thévenin port equivalent.*

A suitable WDF adaptor structure follows from the derived SPQR tree. The second step of our method is to find the scattering behavior of each adaptor in the SPQR tree. The scattering behavior of series and parallel adaptors is well-known [19], but the actual scattering behavior of $\mathcal{R}$-type adaptors is not. We require an easy-to-apply technique that yields this scattering behavior for any $\mathcal{R}$-type adaptor, even ones including absorbed multiport linear elements, and that allows us to make one port *reflection-free* to ensure computability of the WDF structure.

Our novel method accomplishes these goals within the framework of the Modified Nodal Analysis (MNA) formalism [9, 10]. Since MNA works in the Kirchhoff domain, we need to form an equivalent circuit that corresponds to adaptor port definitions. We call the circuit which produces a certain incident wave upon a port an *instantaneous Thévenin port equivalent*.[3] It is easily derived by considering the relationships among a voltage source value e, source current j, electrical resistance R, port voltage v, port current i, port resistance R_p, incident wave a, and reflected wave b.

A single WDF port and its instantaneous Thévenin equivalent are shown in Fig. 1. If we set $R = R_p$, the voltage source value must be equal to the incident wave; $e = a$. In every case, we can see that $i = -j$. This is identical to the classic derivation of adaptation criteria for a resistive voltage source [1], but framing it "backwards" shows us how to create a Kirchhoff-domain equivalent to any topological entity including $\mathcal{R}$-type adaptors. Such an equivalent circuit is simply formed by, each port of an adaptor, attaching an instantaneous Thévenin port equivalent, setting the electrical resistance equal to the port resistance, and setting the voltage source value to the incident wave value.

From this equivalent circuit, we need to assemble a MNA system. In general, a MNA system is set up as

$$\underbrace{\begin{bmatrix}\mathbf{Y} & \mathbf{A}\\ \mathbf{B} & \mathbf{D}\end{bmatrix}}_{\text{MNA matrix } \mathbf{X}} \begin{bmatrix}\boldsymbol{v}_n\\ \boldsymbol{j}\end{bmatrix} = \begin{bmatrix}\boldsymbol{i}_s\\ \boldsymbol{e}\end{bmatrix}, \tag{1}$$

where $\mathbf{X}$ partitions $\mathbf{Y}$, $\mathbf{A}$, $\mathbf{B}$, and $\mathbf{D}$ define the relationship among node voltages $\boldsymbol{v}_n$, voltage source branch currents $\boldsymbol{j}$, current source values $\boldsymbol{i}_s$ and voltage source values $\boldsymbol{e}$ [9, 10]. For $\mathcal{R}$-type adaptors with no linear multiport elements, we will only employ resistor and voltage source stamps, yielding a version of (1) where $\mathbf{B} = \mathbf{A}^\mathsf{T}$ and $\mathbf{D} = \mathbf{0}$. In our context, we will also always have $\boldsymbol{i}_s = 0$.

Finding $\mathbf{X}$ by inspection using, e.g., Kirchhoff's Current Law (KCL) is possible, but can be tedious—the use of *element stamps* (sometimes called "MNA templates" [11, 12] or MNA "by inspection" [10]) greatly simplifies this process, even to the point of being automatable. Using element stamps is simple. Every node in

[3] This is related to the *augmented network* described by Belevitch [29] and has also been called the *Wave Equivalent Thevenin Source* in microstrip engineering [30].

Table 1: *Modified Nodal Analysis element stamps.*

	resistor	voltage source	VCVS
symbol		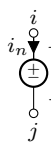	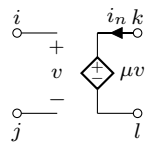
stamp	$\begin{matrix} & i & j \\ i & G & -G \\ j & -G & G \end{matrix}$	$\begin{matrix} & i & j & n & \\ i & & & 1 & \\ j & & & -1 & \\ \text{next} & 1 & -1 & & \end{matrix}$ source $\begin{matrix} \\ \\ \\ \overline{E} \end{matrix}$	$\begin{matrix} & i & j & k & l & n \\ k & & & & & 1 \\ l & & & & & -1 \\ \text{next} & -\mu & \mu & 1 & -1 & \end{matrix}$

the equivalent circuit is assigned an index, and then the contribution of each element is added into $\mathbf{X}$ one by one according to the element stamps. A fine point of this process is that one node in the equivalent circuit is chosen as the "datum" node, and neither its row nor its column appear in $\mathbf{X}$. Since the number of independent KCL equations in a circuit is always one less than the number of nodes [31], $\mathbf{X}$ would always be singular without this step.

Element stamps corresponding to a resistor, a voltage source, and a voltage-controlled voltage source are given in Table 1. Other stamps, corresponding to, e.g., transformers and other controlled sources, are given in the MNA literature [9–11].

A populated MNA system can be used to derive the scattering behavior of an $\mathcal{R}$-type adaptor. Recall the standard WDF voltage wave definition [1], applied to a vector of ports,

$$\boldsymbol{a} = \boldsymbol{v} + \mathbf{R}_p \boldsymbol{i} \quad \text{and} \quad \boldsymbol{b} = \boldsymbol{v} - \mathbf{R}_p \boldsymbol{i}\,, \tag{2}$$

with vectors of incident and reflected waves $\boldsymbol{a}$ and $\boldsymbol{b}$, and a diagonal matrix of port resistances $\mathbf{R}_p$. Combining (2) yields

$$\boldsymbol{b} = \boldsymbol{a} - 2\mathbf{R}_p \boldsymbol{i}\,. \tag{3}$$

Recall that in forming our equivalent circuit we imposed

$$\boldsymbol{e} = \boldsymbol{a}\,, \quad \mathbf{R} = \mathbf{R}_p\,, \quad \text{and} \quad \boldsymbol{i} = -\boldsymbol{j}\,. \tag{4}$$

Inverting $\mathbf{X}$ from (1) allows us to solve for $\boldsymbol{j}$ in terms of $\boldsymbol{e}$:

$$\boldsymbol{j} = \begin{bmatrix}\mathbf{0} & \mathbf{I}\end{bmatrix} \mathbf{X}^{-1} \begin{bmatrix}\mathbf{0} & \mathbf{I}\end{bmatrix}^{\mathsf{T}} \boldsymbol{e}\,. \tag{5}$$

Combining (3), (4), and (5), yields

$$\boldsymbol{b} = \mathbf{S}\boldsymbol{a}\,, \quad \text{with} \quad \mathbf{S} = \mathbf{I} + 2\begin{bmatrix}\mathbf{0} & \mathbf{R}\end{bmatrix} \mathbf{X}^{-1} \begin{bmatrix}\mathbf{0} & \mathbf{I}\end{bmatrix}^{\mathsf{T}}\,. \tag{6}$$

This method is simple to apply and yields a scattering matrix even for adaptors which have absorbed multiport linear elements. In a WDF, we always need to be able to ensure that the port facing towards the root of the tree is reflection free, i.e., the reflected wave at that port does not depend instantaneously on the incident wave at that port. This is accomplished just as in the traditional series and parallel cases. For a port n that we must adapt, we simply solve for the value of R_n which accomplishes $s_{nn} = 0$, where s_{nn} is the diagonal entry of $\mathbf{S}$ corresponding to the contribution of incident wave a_n to reflected wave b_n.

We stress that the adaptors resulting from this process are fully compatible with a standard WDF *tree* framework. It is well-known that N-port series (parallel) adaptors can always be decomposed into $N-2$ cascaded 3-port series (parallel) adaptors [26]. This property means that each adaptor in a Binary Connection Tree

Table 2: $\mathbf{S}_{rings}$ *stamps for series/parallel adaptors.*

	series connection	parallel connection
adaptor	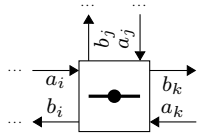	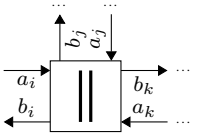
stamp	$\begin{matrix} & i & j & k \\ i & 1-\gamma_i & -\gamma_i & -\gamma_i \\ j & -\gamma_j & 1-\gamma_j & -\gamma_j \\ k & -\gamma_k & -\gamma_k & 1-\gamma_k \end{matrix}$ $\gamma_m = \frac{2R_m}{(R_i+R_j+R_k)}$	$\begin{matrix} & i & j & k \\ i & \delta_i-1 & \delta_j & \delta_k \\ j & \delta_i & \delta_j-1 & \delta_k \\ k & \delta_i & \delta_j & \delta_k-1 \end{matrix}$ $\delta_m = \frac{2G_m}{(G_i+G_j+G_k)}$

Table 3: $\mathbf{C}$ *stamps for port compatibility.*

	direct connection	inverse connection
ports	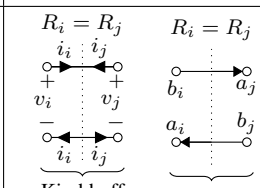	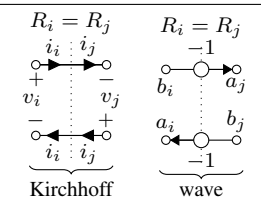
stamp	$\begin{matrix} & i & j \\ i & 0 & 1 \\ j & 1 & 0 \end{matrix}$	$\begin{matrix} & i & j \\ i & 0 & -1 \\ j & -1 & 0 \end{matrix}$

(BCT) [26, 32, 33] always has one parent and two children. However, $\mathcal{R}$-type adaptors cannot be decomposed into smaller adaptors and have $N \geq 6$ ports. Hence they have $N-1 \geq 5$ children and a connection tree including them can no longer be assumed binary. To avoid a loss of generality for circuits with $\mathcal{R}$-type adaptors, we drop the "Binary" from the BCT concept, calling it rather the "Connection Tree" (CT)—this does not require any further alteration to standard WDF theory or terminology.

4. METHOD TWO: "RING" RESOLUTION

The method presented in §3 is simple and systematic and should be applicable to deriving the scattering behavior of *any* WDF adaptor, including hitherto intractable $\mathcal{R}$-type adaptors with or without absorbed multiport linear elements.

In this section, we present an alternate derivation which combines non-tree-like arrangements of standard 3-port series and parallel adaptors which are occasionally seen in the WDF literature [2, 27] into one larger $\mathcal{R}$-type adaptor. These are usually noncomputable since they violate the assumption of a tree structure and hence contain delay-free loops, though recent work achieves guaranteed convergence under runtime iteration [2]. As before, we can render one of the ports in this adaptor reflection-free, making it suitable for inclusion in a standard WDF tree.

We denote the incident and reflected waves at ports that are *internal* to the noncomputable network as $\boldsymbol{a}_i$ and $\boldsymbol{b}_i$ and those that are *external* as our normal wave variables $\boldsymbol{a}$ and $\boldsymbol{b}$ as before. Internal ports face other adaptors within the noncomputable network and external ports face the rest of the WDF structure. The whole

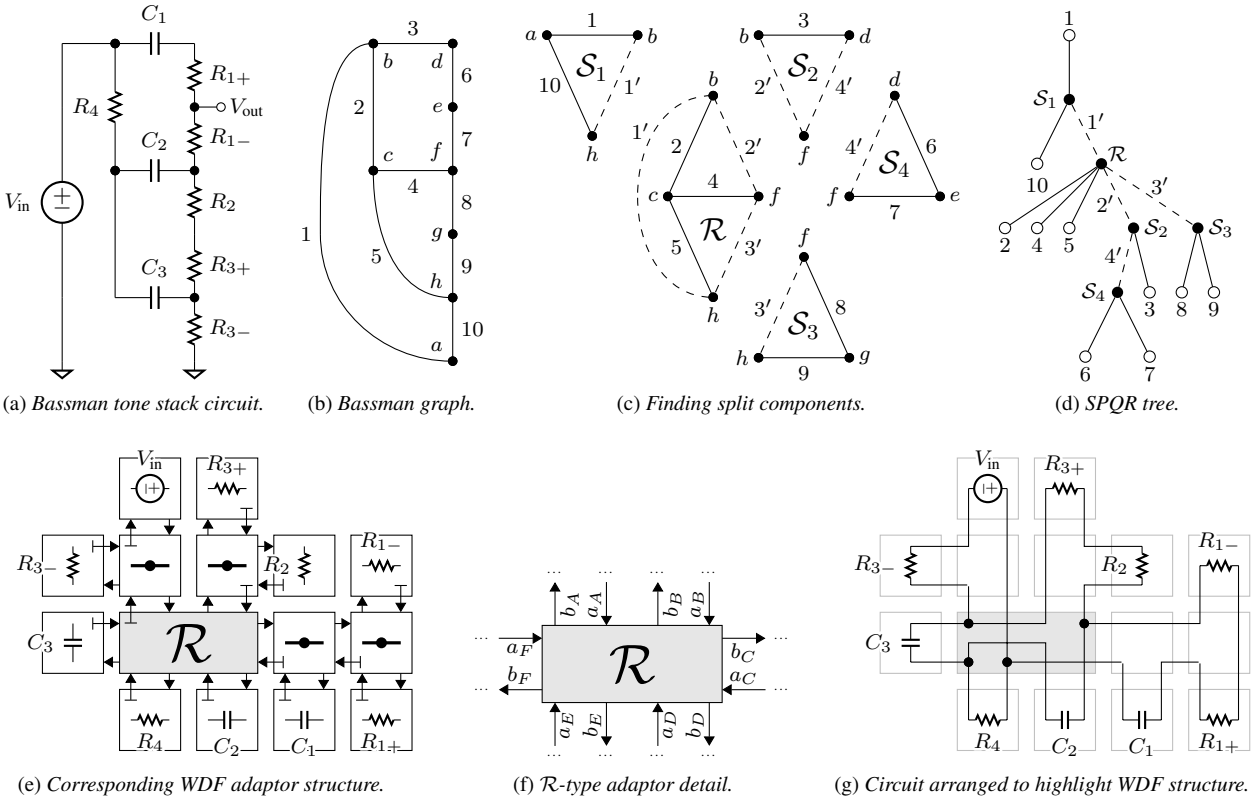

(a) *Bassman tone stack circuit.* (b) *Bassman graph.* (c) *Finding split components.* (d) *SPQR tree.*

(e) *Corresponding WDF adaptor structure.* (f) *$\mathcal{R}$-type adaptor detail.* (g) *Circuit arranged to highlight WDF structure.*

Figure 2: *Deriving a WDF adaptor structure for the Fender Bassman tone stack, as in §3.*

noncomputable structure is described by the scattering description

$$\begin{bmatrix} \boldsymbol{b}_i \\ \boldsymbol{b} \end{bmatrix} = \underbrace{\begin{bmatrix} \mathbf{S}_{11} & \mathbf{S}_{12} \\ \mathbf{S}_{21} & \mathbf{S}_{22} \end{bmatrix}}_{\mathbf{S}_{\text{rings}}} \begin{bmatrix} \boldsymbol{a}_i \\ \boldsymbol{a} \end{bmatrix} . \tag{7}$$

From this description, we need to find $\mathbf{S}$ as in (6). It is not difficult to populate the $\mathbf{S}_{\text{rings}}$ partitions $\mathbf{S}_{11}$, $\mathbf{S}_{12}$, $\mathbf{S}_{21}$, and $\mathbf{S}_{22}$. Since (7) describes the behavior of an interconnected network of *standard* 3-port series and parallel adaptors (albeit a noncomputable one), the *local* scattering behavior is known. Recall the scattering matrices for unconstrained 3-port series and parallel adaptors, with three ports i, j, and k, incident waves a_i, a_j, and a_k, and reflected waves b_i, b_j, and b_k. The scattering at these adaptors is described by resistance and conductance ratios γ_m and δ_m [26, 34].[4] Hence $\mathbf{S}_{11}$, $\mathbf{S}_{12}$, $\mathbf{S}_{21}$, and $\mathbf{S}_{22}$ can be populated by inspection. Taking inspiration from the *Wave Tableau* (WT) technique [33], and to match the simplicity of the MNA element stamp method presented in §3, we introduce a two-part stamp method for populating these matrices. We note that the WT technique is applied globally, while this method leverages graph-theoretic perspectives [24] to restrict the tableau to a minimal subtree. After assigning each port a numerical index, the stamps shown in Table 2 are used to populate (7).

At the internal ports, a port *C*ompatibility matrix $\mathbf{C}$ describes the relationship between $\boldsymbol{a}_i$ and $\boldsymbol{b}_i$:

$$\boldsymbol{a}_i = \mathbf{C}\boldsymbol{b}_i . \tag{8}$$

[4] Recall that conductance is the reciprocal of resistance: $G_m = 1/R_m$.

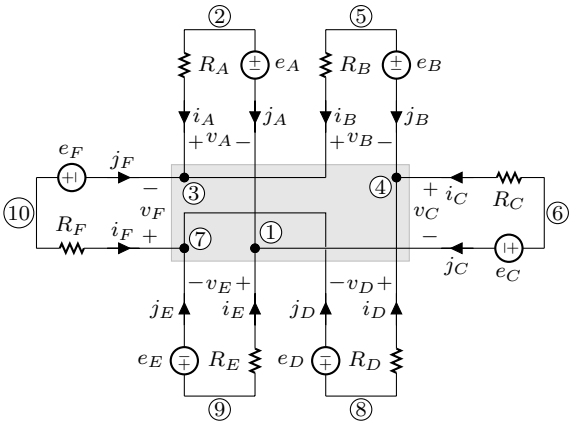

Figure 3: *Instantaneous Thévenin port equivalent to Fig. 2f.*

$\mathbf{C}$ can also be populated by inspection; every internal incident wave is equal to the reflected wave at the port it is connected to, sometimes with a sign inversion if the polarities at that port don't match. $\mathbf{C} = \mathbf{C}^{\mathsf{T}}$ on account of the reciprocity of port connections. We abstract this process into another stamp procedure. Stamps for direct connections and inverse connections[5] are shown in Table 3.

[5] Sometimes known as "null" connections [35], this can also be considered the case of an adapted ($R_i = R_j$) 2-port series adaptor [1].

$$\mathbf{X} = \left[\begin{array}{c|c} \mathbf{Y} & \mathbf{A} \\ \hline \mathbf{B} & \mathbf{D} \end{array}\right] = \begin{array}{c} \\ ② \\ ③ \\ ④ \\ ⑤ \\ ⑥ \\ ⑦ \\ ⑧ \\ ⑨ \\ ⑩ \\ A \\ B \\ C \\ D \\ E \\ F \end{array} \begin{array}{c} \begin{array}{cccccccccccccccc} ② & ③ & ④ & ⑤ & ⑥ & ⑦ & ⑧ & ⑨ & ⑩ & A & B & C & D & E & F \end{array} \\ \left[\begin{array}{cccccccccccccccc} G_A & -G_A & 0 & 0 & 0 & 0 & 0 & 0 & 0 & 1 & 0 & 0 & 0 & 0 & 0 \\ -G_A & G_A+G_B & 0 & -G_B & 0 & 0 & 0 & 0 & 0 & 0 & 0 & 0 & 0 & 0 & -1 \\ 0 & 0 & G_C+G_D & 0 & -G_C & 0 & -G_D & 0 & 0 & 0 & -1 & 0 & 0 & 0 & 0 \\ 0 & -G_B & 0 & G_B & 0 & 0 & 0 & 0 & 0 & 0 & 1 & 0 & 0 & 0 & 0 \\ 0 & 0 & -G_C & 0 & G_C & 0 & 0 & 0 & 0 & 0 & 0 & 1 & 0 & 0 & 0 \\ 0 & 0 & 0 & 0 & 0 & G_F & 0 & 0 & -G_F & 0 & 0 & 0 & -1 & -1 & 0 \\ 0 & 0 & -G_D & 0 & 0 & 0 & G_D & 0 & 0 & 0 & 0 & 0 & 1 & 0 & 0 \\ 0 & 0 & 0 & 0 & 0 & 0 & 0 & G_E & 0 & 0 & 0 & 0 & 0 & 1 & 0 \\ 0 & 0 & 0 & 0 & 0 & -G_F & 0 & 0 & G_F & 0 & 0 & 0 & 0 & 0 & 1 \\ 1 & 0 & 0 & 0 & 0 & 0 & 0 & 0 & 0 & 0 & 0 & 0 & 0 & 0 & 0 \\ 0 & 0 & -1 & 1 & 0 & 0 & 0 & 0 & 0 & 0 & 0 & 0 & 0 & 0 & 0 \\ 0 & 0 & 0 & 0 & 1 & 0 & 0 & 0 & 0 & 0 & 0 & 0 & 0 & 0 & 0 \\ 0 & 0 & 0 & 0 & 0 & -1 & 1 & 0 & 0 & 0 & 0 & 0 & 0 & 0 & 0 \\ 0 & 0 & 0 & 0 & 0 & -1 & 0 & 1 & 0 & 0 & 0 & 0 & 0 & 0 & 0 \\ 0 & -1 & 0 & 0 & 0 & 0 & 0 & 0 & 1 & 0 & 0 & 0 & 0 & 0 & 0 \end{array}\right] \end{array}$$

Figure 4: *Bassman MNA system matrix—example resistor stamp in light shading, example voltage source stamp in dark shading.*

Rearranging (8) as $\boldsymbol{b}_i = \mathbf{C}^{-1}\boldsymbol{a}_i$ and substituting into the top set of equations in (7) yields

$$\mathbf{C}^{-1}\boldsymbol{a}_i = \mathbf{S}_{11}\boldsymbol{a}_i + \mathbf{S}_{12}\boldsymbol{a}\,. \tag{9}$$

Solving for $\boldsymbol{a}_i$ yields

$$\boldsymbol{a}_i = (\mathbf{C}^{-1} - \mathbf{S}_{11})^{-1}\mathbf{S}_{12}\boldsymbol{a}\,. \tag{10}$$

Substituting into the bottom set of equations of (7) yields

$$\mathbf{S} = \mathbf{S}_{21}(\mathbf{C}^{-1} - \mathbf{S}_{11})^{-1}\mathbf{S}_{12} + \mathbf{S}_{22}\,. \tag{11}$$

When it can be applied, this method gives identical results to §3. An advantage is that it does not require any recourse to graph theory. A disadvantage is that noncomputable adaptor structures only arise from inspection—there is no known systematic procedure for generating them. Unlike §3, this technique does not support cases involving multiport linear circuit elements.

5. CASE STUDIES

The results of this paper enable us to model linear circuits which would previously have been off-limits as reference circuits for a WDF. We present two detailed tutorial examples demonstrating our techniques: the tone stack from the Fender Bassman amp and the tone/volume stage from the Tube Screamer distortion pedal.

5.1. Fender Bassman Tone Stack

As a first example, we'll study the tone stack from the Fender Bassman amp[6] (Fig. 2a), using each of the two methods derived in §§3–4. Yeh and Smith studied the Bassman tone stack by deriving its transfer function [4]. Although they suggested that it could potentially be implemented as a WDF, that would have been a daunting task at the time, since the Bassman tone stack circuit (Fig. 2a) can't be decomposed into a tree of series and parallel adaptors. Until now simulation of this circuit as a WDF would require the use of component consolidation [3] or topological transformations such as the Y–Δ ("wye–delta") transformation [36].

What follows is a step by step walkthrough of how §3 can be applied to model this circuit. First a graph representing this circuit is formed (Fig. 2b). In this graph, nodes correspond to circuit nodes and are each assigned a lowercase letter. Graph edges correspond to ports in the circuit and are each assigned an arabic numeral. For this graph representation, we follow the procedure of Fränken *et al.* [24] to find split components (Fig. 2c). This yields four series connections and a 6-port $\mathcal{R}$-type connection. We designate the voltage source (edge 1) as the root of the tree for realizability reasons—an ideal voltage source cannot be adapted and must be a root element. From here, an SPQR tree can be formed (Fig. 2d). A WDF adaptor structure follows by identity from this SPQR tree (Fig. 2e). This adaptor structure contains one $\mathcal{R}$-type adaptor, corresponding to the $\mathcal{R}$-type connection in Fig. 2c. Incident and reflected wave labeling details (each port is assigned a lowercase letter) of this problematic adaptor are shown in detail in Fig. 2f, and a rearranged version of Fig. 2a which highlights the derived adaptor structure is shown in Fig. 2g.

We form an equivalent circuit to Fig. 2f by attaching instantaneous Thévenin port equivalents (Fig. 3). Each node is assigned a circled arabic numeral. Using an MNA stamp (Table 1) for each voltage source and resistor yields the system matrix $\mathbf{X}$ (Fig. 4).

Each stamp contributes to certain entries in the system matrix and source vector. That is, multiple stamps can contribute to the same system matrix entry. For instance, we can see this at play at matrix entries $(③, ③)$ and $(④, ④)$ in Fig. 4.

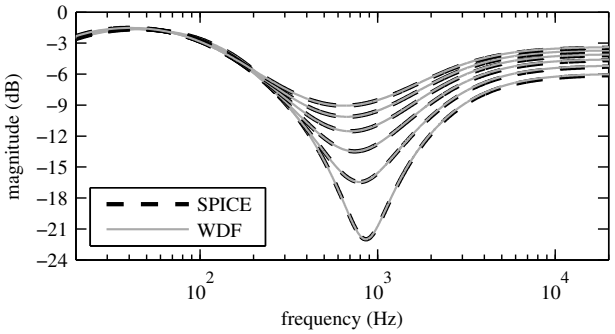

Figure 5: *Bassman magnitude responses, low and high potentiometers at* 50%*, mid potentiometer at* 20% *increments.*

[6] R_1, R_2, and R_3 are high, low, and mid tone control potentiometers.

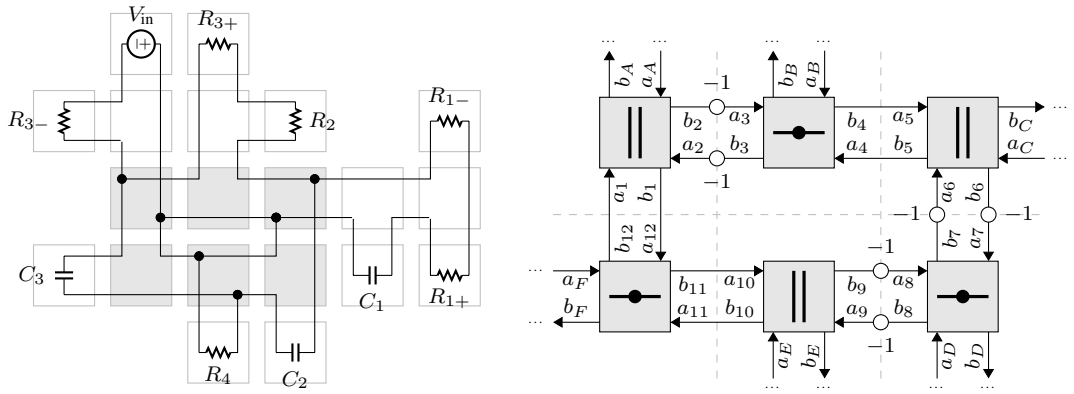

(a) *Circuit arranged using only series/parallel connections.* (b) *Detail on noncomputable system of series/parallel adaptors.*

Figure 6: *Considering Bassman tone stack with only series/parallel adaptors, as in §4.*

Plugging Fig. 4 into (6) yields the scattering matrix $\mathbf{S}$ of this adaptor. Since port A is facing towards the root of the WDF tree, it must be rendered reflection-free. This is accomplished by solving for the value of R_A which sets $s_{11} = 0$.

To verify this model, we compare a family of magnitude response curves to "ground truth" SPICE simulations (Fig. 5). We find the WDF magnitude responses by taking the FFT of an impulse response that has sufficiently decayed to zero. The WDF magnitude response shows a close correspondence to SPICE, except for the expected frequency warping at high frequencies, a known property of the bilinear transform (BLT) [21].[7]

We can also use the Bassman tone stack as an example of §4. Rather than using the SPQR technique of Fränken *et al.*, we create (by inspection) an adaptor structure that only uses series and parallel adaptors (Fig. 6a). This is similar to Fig. 2e, but the $\mathcal{R}$ node of Fig. 2e has been replaced by a noncomputable network of series and parallel adaptors, shown in detail in Fig. 6b.

Denoting the length-6 vectors of external incident and reflected waves as $\boldsymbol{a} = [a_A, \ldots, a_F]^\mathsf{T}$ and $\boldsymbol{b} = [b_A, \ldots, b_F]^\mathsf{T}$ and the length-12 vectors of internal incident and reflected waves as $\boldsymbol{a}_i = [a_1, \ldots, a_{12}]^\mathsf{T}$ and $\boldsymbol{b}_i = [b_1, \ldots, b_{12}]^\mathsf{T}$, we apply the stamp procedures of §4. The matrix resulting from the stamp procedure (Table 2) is given in Fig. 7. The compatibility matrix (8) relating $\boldsymbol{a}_i$ and $\boldsymbol{b}_i$ is found according to the next stamp procedure (Table 3):

$$\mathbf{C} = \begin{array}{c} \begin{array}{cccccccccccc} 1 & 2 & 3 & 4 & 5 & 6 & 7 & 8 & 9 & 10 & 11 & 12 \end{array} \\ \left[\begin{array}{cccccccccccc} 0 & 0 & 0 & 0 & 0 & 0 & 0 & 0 & 0 & 0 & 0 & 1 \\ 0 & 0 & -1 & 0 & 0 & 0 & 0 & 0 & 0 & 0 & 0 & 0 \\ 0 & -1 & 0 & 0 & 0 & 0 & 0 & 0 & 0 & 0 & 0 & 0 \\ 0 & 0 & 0 & 0 & 1 & 0 & 0 & 0 & 0 & 0 & 0 & 0 \\ 0 & 0 & 0 & 1 & 0 & 0 & 0 & 0 & 0 & 0 & 0 & 0 \\ 0 & 0 & 0 & 0 & 0 & 0 & -1 & 0 & 0 & 0 & 0 & 0 \\ 0 & 0 & 0 & 0 & 0 & -1 & 0 & 0 & 0 & 0 & 0 & 0 \\ 0 & 0 & 0 & 0 & 0 & 0 & 0 & -1 & 0 & 0 & 0 & 0 \\ 0 & 0 & 0 & 0 & 0 & 0 & 0 & 0 & -1 & 0 & 0 & 0 \\ 0 & 0 & 0 & 0 & 0 & 0 & 0 & 0 & 0 & 0 & 1 & 0 \\ 0 & 0 & 0 & 0 & 0 & 0 & 0 & 0 & 0 & 1 & 0 & 0 \\ 1 & 0 & 0 & 0 & 0 & 0 & 0 & 0 & 0 & 0 & 0 & 0 \end{array}\right] \end{array}. \quad (12)$$

Here light shading indicates one example of an inverse connection and dark shading indicates one example of a direct connection. Plugging Fig. 7 and (12) into (11) yields an identical $\mathbf{S}$ to that obtained by the previous method.

[7] `https://ccrma.stanford.edu/~jos/pasp/Bilinear_Transformation.html`

5.2. Tube Screamer Tone/Volume Stage

As a second case study, we derive a WDF from the tone/volume stage of the Tube Screamer distortion pedal.[8] This derivation is similar to §5.1, although somewhat complicated by the op-amp. In addition to showing a case where an adaptor "absorbs" a linear multiport element, this demonstrates how these techniques can be used for advanced and general op-amp modeling. Unlike [8], this technique is not limited to differential amplifier arrangements.

In the circuit (Fig. 8a), the op-amp is treated as ideal, i.e., as a voltage-controlled voltage source that relates the output voltage to the differential input voltage $v_+ - v_-$ by a large open-loop gain A_{OL}. A graph (Fig. 8b) is formed by the *replacement graph* method of Fränken *et al.* [24]; nameless replacement graph nodes and edges are indicated in gray. Detail on the resulting $\mathcal{R}$-type topology is shown in Fig. 8c; remaining standard series and parallel structures are not shown. As before, the split component search yields an SPQR tree (Fig. 8d) and corresponding WDF adaptor structure (Fig. 8e). Notice in Fig. 8f that the controlled source has been absorbed into the $\mathcal{R}$-type adaptor. The $\mathcal{R}$-type adaptor scattering matrix derivation is done according to §3.

To verify this model, we compare a family of magnitude response curves to "ground truth" SPICE simulations (Fig. 9). The WDF magnitude response shows an excellent correspondence to SPICE, except for BLT frequency warping as before.

6. CONCLUSION

We presented a method (§3) that leverages Modified Nodal Analysis to derive the scattering behavior of WDF adaptors with complicated topologies and even absorbed multiport linear elements. This method is applicable to reference circuits involving any multi-port linear elements with MNA descriptions, e.g., voltage- or current-controlled voltage or current sources and transformers. A second method (§4), applicable to non-tree-like combinations of series and parallel adaptors, involves algebraic wave domain manipulations. Both are based on simple stamp philosophies and yield adaptors which are suitable for inclusion in standard WDF trees. Combining these methods with the graph-theoretic insights of Fränken *et al.* brings a high degree of generality to linear WDFs.

[8] R_2 and R_3 are tone and volume control potentiometers.

$$\mathbf{S}_{\text{rings}} = \left[\begin{array}{c|c} \mathbf{S}_{11} & \mathbf{S}_{12} \\ \hline \mathbf{S}_{21} & \mathbf{S}_{22} \end{array}\right] = \ldots$$

	1	2	3	4	5	6	7	8	9	10	11	12	A	B	C	D	E	F
1	δ_1-1	δ_2	0	0	0	0	0	0	0	0	0	0	δ_A	0	0	0	0	0
2	δ_1	δ_2-1	0	0	0	0	0	0	0	0	0	0	δ_A	0	0	0	0	0
3	0	0	$1-\gamma_3$	$-\gamma_3$	0	0	0	0	0	0	0	0	0	$-\gamma_3$	0	0	0	0
4	0	0	$-\gamma_4$	$1-\gamma_4$	0	0	0	0	0	0	0	0	0	$-\gamma_4$	0	0	0	0
5	0	0	0	0	δ_5-1	δ_6	0	0	0	0	0	0	0	0	δ_C	0	0	0
6	0	0	0	0	δ_5	δ_6-1	0	0	0	0	0	0	0	0	δ_C	0	0	0
7	0	0	0	0	0	0	$1-\gamma_7$	$-\gamma_7$	0	0	0	0	0	0	0	$-\gamma_7$	0	0
8	0	0	0	0	0	0	$-\gamma_8$	$1-\gamma_8$	0	0	0	0	0	0	0	$-\gamma_8$	0	0
9	0	0	0	0	0	0	0	0	δ_9-1	δ_{10}	0	0	0	0	0	0	δ_E	0
10	0	0	0	0	0	0	0	0	δ_9	$\delta_{10}-1$	0	0	0	0	0	0	δ_E	0
11	0	0	0	0	0	0	0	0	0	0	$1-\gamma_{11}$	$-\gamma_{11}$	0	0	0	0	0	$-\gamma_{11}$
12	0	0	0	0	0	0	0	0	0	0	$-\gamma_{12}$	$1-\gamma_{12}$	0	0	0	0	0	$-\gamma_{12}$
A	δ_1	δ_2	0	0	0	0	0	0	0	0	0	0	δ_A-1	0	0	0	0	0
B	0	0	$-\gamma_B$	$-\gamma_B$	0	0	0	0	0	0	0	0	0	$1-\gamma_B$	0	0	0	0
C	0	0	0	0	δ_5	δ_6	0	0	0	0	0	0	0	0	δ_C-1	0	0	0
D	0	0	0	0	0	0	$-\gamma_D$	$-\gamma_D$	0	0	0	0	0	0	0	$1-\gamma_D$	0	0
E	0	0	0	0	0	0	0	0	δ_9	δ_{10}	0	0	0	0	0	0	δ_E-1	0
F	0	0	0	0	0	0	0	0	0	0	$-\gamma_F$	$-\gamma_F$	0	0	0	0	0	$1-\gamma_F$

Figure 7: *Bassman loop resolution matrix—example parallel stamp in light shading, example series stamp in dark shading.*

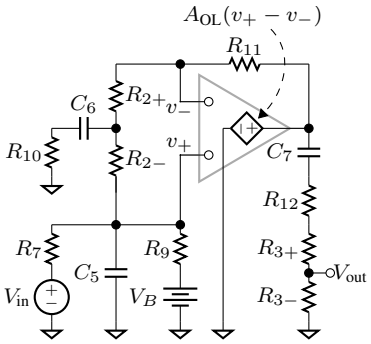

(a) *Tube Screamer tone/volume stage circuit.*

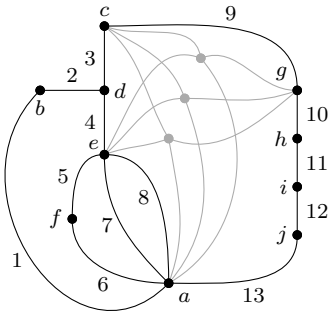

(b) *Tube Screamer graph.*

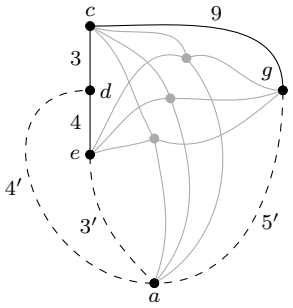

(c) *Finding split components.*

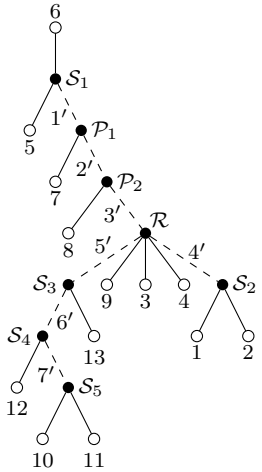

(d) *SPQR tree.*

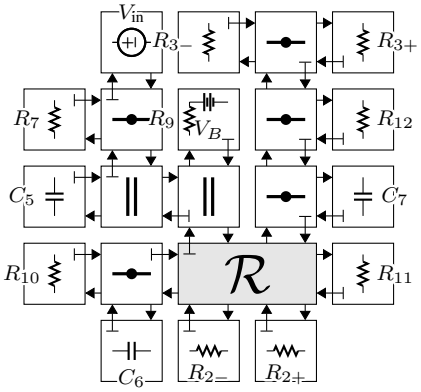

(e) *Corresponding WDF adaptor structure.*

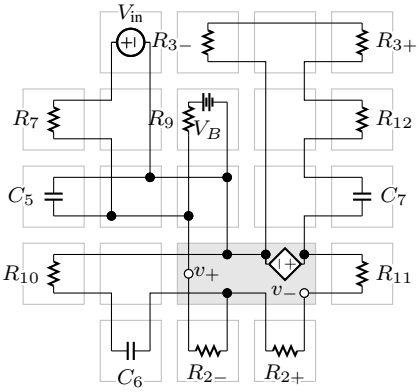

(f) *Circuit arranged to highlight WDF structure.*

Figure 8: *Deriving a WDF adaptor structure for the Tube Screamer tone/volume stage, as in §3.*

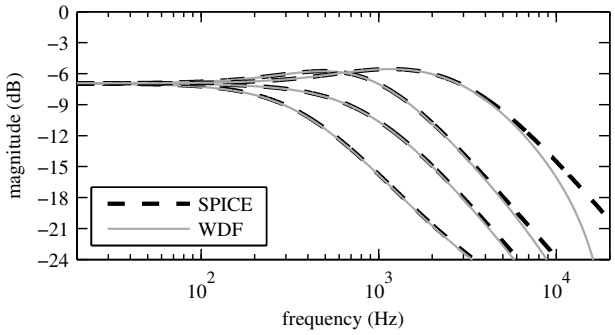

Figure 9: *Tube Screamer magnitude responses, volume potentiometer at* 50%*, tone potentiometer at* 0%*,* 50%*,* 95%*, and* 100%*.*

In general, adapted n-port scattering matrices involve $n^2 - 1$ multiplies. One-multiplier realizations of 2- and 3-port adaptors are well known [1, 3]. Even without exploiting any structural knowledge of scattering matrices, it may be possible to reduce realization cost with matrix factorization [25]. Future work should seek canonic realizations of the adaptors presented in this paper.

We've focused on lingering issues of topology in WDF models of *linear* reference circuits. The presented methods are applicable to the same situations in nonlinear circuits. Computability concerns greatly heighten topological issues for WDF models of reference circuits with multiple/multiport nonlinearities. A companion paper [14] expands on the initial perspective of [28] and shows how the methods in this paper can yield a novel framework for considering WDFs with multiple/multiport nonlinear elements.

7. REFERENCES

[1] A. Fettweis, "Wave digital filters: Theory and practice," *Proc. IEEE*, vol. 74, no. 2, pp. 270–327, 1986.

[2] T. Schwerdtfeger and A. Kummert, "A multidimensional signal processing approach to wave digital filters with topology-related delay-free loops," in *Proc. IEEE Int. Conf. Acoust., Speech Signal Process. (ICASSP)*, Florence, Italy, May 4–9 2014, pp. 389–393.

[3] M. Karjalainen, "Efficient realization of wave digital components for physical modeling and sound synthesis," *IEEE Trans. Audio, Speech, Language Process.*, vol. 16, no. 5, pp. 947–956, 2008.

[4] D. T.-M. Yeh and J. O. Smith III, "Discretization of the '59 Fender Bassman tone stack," in *Proc. Int. Conf. Digital Audio Effects (DAFx-06)*, Montréal, Canada, Sept. 18–20 2006.

[5] K. J. Werner et al., "A physically-informed, circuit-bendable, digital model of the Roland TR-808 bass drum circuit," in *Proc. Int. Conf. Digital Audio Effects*, Erlangen, Germany, Sept. 1–5 2014, vol. 17.

[6] K. J. Werner et al., "The TR-808 cymbal: a physically-informed, circuit-bendable, digital model," in *Proc. Int. Comput. Music / Sound Music Comput. Conf.*, Athens, Greece, Sept. 14–20 2014, vol. 40/11.

[7] K. J. Werner et al., "More cowbell: a physically-informed, circuit-bendable, digital model of the TR-808 cowbell," in *Proc. Int. Audio Eng. Soc. (AES) Conv.*, Los Angeles, CA, Oct. 9–12 2014, vol. 137.

[8] R. C. D. Paiva et al., "Emulation of operational amplifiers and diodes in audio distortion circuits," *IEEE Trans. Circuits Syst. II: Expr. Briefs*, vol. 59, no. 10, pp. 688–692, 2012.

[9] C.-W. Ho et al., "The modified nodal approach to network analysis," *IEEE Trans. Circuits Syst*, vol. 22, no. 6, pp. 504–509, 1975.

[10] J. Vlach and K. Singhal, *Computer methods for circuit analysis and design*, Springer, 1983.

[11] D. T.-M. Yeh et al., "Automated physical modeling of nonlinear audio circuits for real-time audio effects—part I: Theoretical development," *IEEE Trans. Audio, Speech, Language Process.*, vol. 18, no. 4, pp. 728–737, 2010.

[12] D. T.-M. Yeh, "Automated physical modeling of nonlinear audio circuits for real-time audio effects—part II: BJT and vacuum tube examples," *IEEE Trans. Audio, Speech, Language Process.*, vol. 20, no. 4, pp. 1207–1216, 2012.

[13] K. Meerkötter and R. Scholz, "Digital simulation of nonlinear circuits by wave digital filter principles," in *Proc. IEEE Int. Symp. Circuits Syst.*, June 1989, vol. 1, pp. 720–723.

[14] K. J. Werner et al., "Resolving wave digital filters with multiple/multiport nonlinearities," in *Proc. Int. Conf. Digital Audio Effects (DAFx-15)*, Trondheim, Norway, Nov. 30 – Dec. 3 2015.

[15] A. Fettweis, "Some principles of designing digital filters imitating classical filter structures," *IEEE Trans. Circuit Theory*, vol. 18, no. 2, pp. 314–316, 1971.

[16] A. Fettweis, "Digital filters structures related to classical filter networks," *Archiv Elektronik Übertragungstechnik (AEÜ)*, vol. 25, pp. 79–89, 1971.

[17] A. Sedlmeyer and A. Fettweis, "Digital filters with true ladder configuration," *Int. J. Circuit Theory Appl.*, vol. 1, pp. 5–10, 1973.

[18] A. Fettweis et al., "Wave digital lattice filters," *Int. J. Circuit Theory Appl.*, vol. 2, pp. 203–211, 1974.

[19] A. Fettweis and K. Meerkötter, "On adaptors for wave digital filters," *IEEE Trans. Acoust., Speech, Signal Process.*, vol. 23, no. 6, 1975.

[20] S. Bilbao, *Wave and Scattering Methods for Numerical Simulation*, John Wiley and Sons, New York, July 2004.

[21] J. O. Smith III, *Physical Audio Signal Processing for Virtual Musical Instruments and Audio Effects*, online book, 2010 edition.

[22] G. O. Martens and K. Meerkötter, "On N-port adaptors for wave digital filters with application to a bridged-tee filter," in *Proc IEEE Int. Symp. Circuits Syst.*, Munich, Germany, Apr. 1976, pp. 514–517.

[23] D. Fränken et al., "Generation of wave digital structures for connection networks containing ideal transformers," in *Proc. Int. Symp. Circuits Syst. (ISCAS '03)*, May 25–28 2003, vol. 3, pp. 240–243.

[24] D. Fränken et al., "Generation of wave digital structures for networks containing multiport elements," *IEEE Trans. Circuits Syst. I: Reg. Papers*, vol. 52, no. 3, pp. 586–596, 2005.

[25] K. Meerkötter and D. Fränken, "Digital realization of connection networks by voltage-wave two-port adaptors," *Archiv Elektronik Übertragungstechnik (AEÜ)*, vol. 50, no. 6, pp. 362–367, 1996.

[26] G. De Sanctis and A. Sarti, "Virtual analog modeling in the wave-digital domain," *IEEE Tran. Audio, Speech, Language Process.*, vol. 18, no. 4, pp. 715–727, 2010.

[27] G. De Sanctis, "Una nuova metodologia per l'implementazione automatica di strutture ad onda numerica orientata alla modellazione ad oggetti di interazioni acustiche," M.S. thesis, Politecnico di Milano, Italy, 2002.

[28] K. J. Werner et al., "A general and explicit formulation for wave digital filters with multiple/multiport nonlinearities and complicated topologies," in *Proc. IEEE Workshop Appl. Sig. Process. Audio Acoust. (WASPAA)*, New Paltz, NY, Oct. 18–21 2015.

[29] V. Belevitch, *Classical network theory*, San Francisco, CA, 1968.

[30] B. P. Stošić and M. V. Gmitrović, "Equivalent Thevenin source method as tool for response calculation of wave digital structures," in *Proc. Int. Conf. Telecommun. Modern Satellite, Cable, Broadcast. Services*, Niš, Serbia, Sept. 26–28 2007, vol. 8, pp. 203–206.

[31] S. Seshu and M. B. Reed, *Linear graphs and electrical networks*, Addison–Wesley, Reading, MA, 1961.

[32] G. De Sanctis et al., "Automatic synthesis strategies for object-based dynamical physical models in musical acoustics," in *Proc. Int. Conf. Digital Audio Effects*, London, UK, Sept. 8–11 2003, vol. 6.

[33] A. Sarti and G. De Sanctis, "Systematic methods for the implementation of nonlinear wave-digital structures," *IEEE Trans. Circuits Syst. I: Reg. Papers*, vol. 56, no. 2, pp. 460–472, 2009.

[34] S. D'Angelo, *Virtual Analog Modeling of Nonlinear Musical Circuits*, Ph.D. diss., Aalto University, Espoo, Finland, Sept. 2014.

[35] S. D'Angelo and V. Välimäki, "Wave-digital polarity and current inverters and their application to virtual analog audio processing," in *Proc. IEEE Int. Conf. Acoust., Speech, Signal Process. (ICASSP)*, Kyoto, Japan, Mar. 2012, pp. 469–472.

[36] D. T.-M. Yeh, "Tutorial on wave digital filters," `https://ccrma.stanford.edu/~dtyeh/papers/wdftutorial.pdf`, Jan. 25 2008.